CrN/NbN coatings deposited by HIPIMS: A preliminary study of erosion-corrosion performance

PURANDARE, Y. P., EHIASARIAN, A. P., STACK, M. M. and HOVSEPIAN, P. E.

Published version

PURANDARE, Y. P., EHIASARIAN, A. P., STACK, M. M. and HOVSEPIAN, P. E. (2010). CrN/NbN coatings deposited by HIPIMS: A preliminary study of erosion-corrosion performance. Surface and coatings technology, 204 (8), 1158-1162.

CrN/NbN coatings deposited by HIPIMS: a preliminary study of erosion-corrosion performance.

PURANDARE, Yashodhan, EHIASARIAN, Arutiun, STACK, Margaret and HOVSEPIAN, Papken

CrN/NbN coatings deposited by HIPIMS: a preliminary study of erosion-corrosion performance.

*Y.P. Purandare [a], A. P. Ehiasarian[a], M.M. Stack[b] and P. Eh. Hovsepian[a].

[a] Materials and Engineering Research Institute,
Sheffield Hallam University, Sheffield,
United Kingdom, S1 1WB.
Tel:+ 44 -114-225 3469
Fax: + 44 - 114-225 3501
Email: y.purandare@shu.ac.uk

[b] Department of Mechanical Engineering,
Strathclyde University, Glasgow,
United Kingdom, G1 1XJ.

Abstract

Nanoscale CrN/NbN multilayer PVD coatings have exhibited resistance to erosion-corrosion. However growth defects (under dense structures and droplets) in the coating produced by some deposition technologies reduce the ability to offer combined erosion-corrosion resistance. In this work a novel High Power Impulse Magnetron Sputtering (HIPIMS) technique has been utilised to pretreat substrates and deposit dense nanoscale CrN/NbN PVD coatings (HIPIMS-HIPIMS technique). This new technique, rich with metal ion plasma, deposits very dense structures and offers virtually defect free coatings (free of droplets as observed in Cathodic Arc technique and under-dense structures observed in standard dc sputtering). Plasma diagnostic studies revealed a high metal ion to gas ion ratio (Cr: Ar) of 3:1

for HIPIMS pretreatment conditions with the detection of 14% Cr^{2+} and 1% Cr^{3+} ions and J_s of 155 $mAcm^{-2}$. For deposition conditions the metal ion to gas ion ratio was approximately 1:4 which is significantly higher compared to DC at 1:30. Characterisation results revealed a high adhesion of L_C 80 N, high hardness of 34 GPa and Young's modulus of 381 GPa. Low friction coefficient (0.46) and dry sliding wear coefficient, K_C (1.22 x 10^{-15} m^3Nm^{-1}) were recorded. The effect of deposition technique (droplet defect and intergranular void free coatings) on erosion-corrosion resistance of CrN/ NbN coatings has been evaluated by subjecting the coatings to a slurry impingement (Na_2CO_3+ $NaHCO_3$ buffer solution with Al_2O_3 particles of size 500-700 µm) at 90^o impact angle with a velocity of 4 ms^{-1}. Experiments have been carried at -1000 mV, +300 mV and +700 mV representing 3 different corrosion conditions.

Keywords: nanoscale, HIPIMS, ionisation, CrN/NbN, erosion-corrosion, slurry impingment.

1.0 Introduction:

Combined erosion-corrosion presents a serious issue for engineering components exposed to corrosive slurries. For example pump impellers, valves and nozzles which encounter corrosive solutions with suspended hard particles show catastrophic failures under this combined attack [1]. Erosion-corrosion analysis of PVD coatings has become more significant with PVD coatings achieving new horizons in the automotive and aerospace sector. CrN/NbN PVD coatings have been developed to achieve high wear and corrosion resistance [2]. These coatings were deposited by the ABS^{TM} technology (Cathodic Arc pretreatment + Unbalanced Magnetron Sputtering (UBM) coating) [3] and were found effective in reducing erosion-corrosion losses more effectively compared with the uncoated substrates [4]. However droplet defects in the coating compromised their effectiveness in resisting erosion-corrosion [5]. The novel High Power Impulse Magnetron Sputtering (HIPIMS) technology has shown to deposit dense, growth defect (voids) free coatings [6-7]. They have superior corrosion [7- 8] and wear resistance [7, 9]. However, their performance under tribo-corrosive conditions has not been analysed to date. This work addresses the issue by studying the effect of HIPIMS technology on the combined erosion-corrosion resistance offered by the nanoscale CrN/NbN coatings. The performance is compared with the coatings deposited by the UBM technology.

2.0 Experimentation:

2.1: Deposition:

Nanoscale multilayer CrN/NbN PVD coatings were deposited in an industrial size Hauzer HTC 1000-4 system enabled with HIPIMS power supply [Hüttinger Elektronic Sp. z o.o., Poland]. Deposition process involved a substrate pretreatment step with HIPIMS plasma discharge enriched with Cr ions [10], followed by deposition of the CrN base layer (using 1 target in HIPIMS mode and 1 target in UBM mode) and then deposition of alternate nanolayers of CrN and NbN to form a multilayered coating. For the nanoscale multilayer

coating step, one chromium target was running in HIPIMS mode whereas other 3 targets (1 Cr and 2 Nb) were running in UBM mode. This technique of deposition using HIPIMS for pretreatment and for coating deposition is henceforth referred as HIPIMS-HIPIMS coating (H-H). For comparison, substrates pretreated with HIPIMS and coating (base layer and nanoscale multilayer) deposited by UBM technology without using HIPIMS (henceforth referred as UBM coating) have been analysed. Coatings were deposited on 1 micron finished M2 high speed steel (HSS) and 304L stainless steel coupons.

2.2 Characterisation:

Relative concentrations of gas ions (Ar^+) and metal ions in the HIPIMS plasma were investigated by an energy-resolved mass spectrometer (PSM003-Hideb Analytical). Time-averaged results were recorded in a Kurt J Lesker CMS-18 sputtering machine equipped with 3 inch cathodes. The surface pretreatment conditions such as Ar pressure, total pressure, target power and current densities were maintained close to that used in the Hauzer HTC1000-4 machine. Details of the setup can be found elsewhere [11]. Ion current densities at the substrates (J_s) during the pretreatment were recorded in the Hauzer HTC1000-4 machine with a flat probe.

The coatings were characterised in terms of their structural, mechanical and tribological properties with a number of analytical techniques. These include scratch adhesion test (CSM-REVETEST) for determination of critical load (L_{C2} according to BS EN 1071-3 standard), ball cratering (CSEM CALOWEAR) for thickness measurement, micro-hardness tests (MITOTOYO Hardness tester) and nano-hardness tests (CSM Nano-hardness tester). The sliding wear coefficients (CSM TRIBOMETER) were calculated by subjecting the specimens at a linear velocity of 0.1 ms^{-1} sliding against a 6 mm Al_20_3 ball for a distance of 3769 m (60,000 laps) under normal load of 5N. X-Ray Diffraction techniques [PAN Analytical

Instruments] such as low angle Bragg-Brentano technique (2θ, 1°-10°) was used for bi-layer period measurement whereas glancing angle technique (2, 2θ, 20-100°) was used for stress analysis [12]. Surface morphology was studied by scanning electron microscopy (NOVA-NanoSEM). Coating microstructure was observed by transmission electron microscopy (Phillips EM 420). Erosion-corrosion volume loss was measured with a stylus profilometer (DEKTAK 150) having a resolution of 33 nm.

2.3 Erosion-corrosion analysis:

Erosion-corrosion performance of the coatings was analysed by subjecting the specimens to an impinging slurry jet at an ambient temperature of 25°C. The details of the apparatus and its operating principle have been described in previous publications [4, 13]. The impinging jet consisted of a slurry of Na_2CO_3+$NaHCO_3$ (buffer solution, pH=10) and 500-700 µm irregular shaped Al_2O_3 particles (7% mass concentration) with a velocity of 4 ms^{-1} impacting at an approach angle of 90° to the specimen surface. To analyse the effect of different corrosion conditions on the erosion-corrosion (combined) material loss, experiments were conducted at 3 different electrochemical potentials of -1000 mV (cathodic), +300 mV (passivating) and +700 mV (anodic). The specimens were masked to preferentially expose 3 x 10^{-5} m^2 area of the specimen.

3.0 Results and discussion:

More noble elements such as Nb in the coating can increase the corrosion resistance to a large extent however its performance in tribo-corrosive conditions will depend on the interaction of the different phases (hard and corrosion resistant phases) present in the coating. Previous work demonstrated that CrN/NbN deposited by the ABS^{TM} technology were effective in providing erosion-corrosion resistance [4, 14]. However results indicated that the droplet defects (generated in the CA pretreatment) in the coating played a significant role in

influencing the extent of protection the coatings can offer. These defects not only allowed the solution a direct path to the substrate but also are the "weak" parts in the coating which form the initiation points of mechanical failure [5].

The novel HIPIMS technology provides an effective way of achieving the desired effects of Arc deposition technology without the macro droplet defects [5, 7]. HIPIMS plasmas are rich in metal ions which when guided towards the substrates can be used for effective sputter cleaning of the substrates as well as to deposit very dense structures. Hence growth defects such as inter-columnar voids, commonly associated with conventional magnetron sputtering, can be avoided with additional benefits of flat and sharp interfaces in the multilayer structure however at lower bias or no bias voltages [15].

3.1Plasma studies:

Plasma diagnostic studies were performed by operating a Cr target in HIPIMS mode with conditions simulating the pretreatment step. In these conditions, the plasma was found to be dominated by Cr^{1+} ions with a relative content of 65%. A significant observation is the presence of Cr^{2+} and Cr^{3+} ions, making a combined relative percentage of 15%. Along with Ar^{1+} ions (23%) Ar^{2+} ions (1.8%) were also observed. Thus HIPIMS has a high percentage of metal ion-to-gas ion ratio of approximately 3:1 which makes the discharge an effective tool for interface engineering, (etching and low energy ion implantation). During the pretreatment step a peak substrate current density (J_s) of 155 $mAcm^{-2}$ was recorded which further confirms the efficiency of ion bombardment. More details on the mass spectroscopy results for the HIPIMS plasma in Ar atmosphere can be found in a previous publication [15].

3.2 Characterisation results:

Table 1

H-H and the UBM coatings had an overall average thickness in the range of 3.9 µm. Coatings deposited by both technologies exhibited a high adhesion value of L_C=80N. Table 1 summarises results obtained from the mechanical testing. As observed, hardness of the H-H coating was higher ($HK_{0.25N}$ = 3393) as compared to the UBM coating ($HK_{0.25N}$ = 3001). XRD measurements revealed that the coatings were under compressive stress with values of - 4.72 GPa and - 1.59 GPa for the H-H and UBM coatings respectively. Also it is evident from the XRD results that bi-layer period of the H-H coating is higher (4.51 nm) than that of the UBM coating (2.38 nm). The friction coefficient value of the H-H coatings (µ= 0.46) was found lower than that of the UBM deposited coating (µ = 0.90). The sliding wear coefficient of the H-H coating was also found lower by a factor of two as compared to the UBM deposited. Enhanced hardness and sliding wear resistance in the HIPIMS deposited coatings has been attributed to the flat and sharp interfaces within the multilayer structure and a dense coating structure without inter-columnar voids obtained as a result of low energy ion bombardment during coating growth in HIPIMS discharge [15]. This improved structure can be seen in Figure 1(a) which is a low magnification (18600 X) bright field TEM image of a cross-section of the CrN/NbN deposited by H-H. The 0.45µm CrN base layer grown on a clean and sharp interface is evident, which is a fingerprint of the HIPIMS pretreatment [16]. Higher hardness of H-H coating can also be attributed to higher residual stresses and bi-layer thickness. The results are consistent with the literature, where hardness of the multilayer coatings has shown an increase with bi-layer thickness (up to a critical value) [17]. The overall coating structure was found to be dense without inter-columnar voids. Absence of macro-droplets and with very flat column tops resulted in low surface roughness values as compared to Arc deposited coatings. Further evidence of the effect of high ion irradiation can be seen in the TEM bright field image at higher magnification (86000 X), figure 1(b), where the alternating CrN and

NbN nanolayers have flat and sharp interfaces and show low layer waviness. In the current study HIPIMS deposited coatings show slightly higher roughness values as compared to the UBM deposited coating which can be attributed to the chamber dust deposited during the coating step.

Figure 1a and 1b.

3.3 Erosion-corrosion results:

In previous studies [4], the nanoscale CrN/NbN multilayer coatings exhibited typical 'brittle' type erosion behaviour [18] with maximum mass loss for particles impacting at 90°. Hence in this study the specimens were subjected to particles impinging at 90° to simulate adverse conditions of testing. Figure 2 shows the polarisation curves obtained by subjecting the H-H and UBM coated substrates at $4ms^{-1}$ under slurry impingement conditions. As observed in the figure, the E-corr value (electrochemical potentials indicating beginning of corrosion) for the H-H coated substrate is marginally noble than the UBM coated substrate. Pretreatment of substrates by the HIPIMS can lead to the incorporation of low energy ions into the substrate [16] and hence to increased corrosion resistance [8]. In this work, in both coating technologies, substrates were pretreated by self bombarding ions from the HIPIMS plasma and hence this can explain the near consistent E-corr values obtained under constant particle bombardment.

Figure 2

UBM deposited coating shows significantly higher corrosion current densities in the electrochemical potential range of -400 mV to + 600 mV. The superior performance of H-H coated substrates in the potential range -400 mV to +600 mV is notable especially when the coating thicknesses were same. These results also suggest that the coating removal rate, and consequently the corrosion rate, for the H-H coating was lower than the UBM coating. This enhanced tribo-corrosion resistance of H-H coating can be attributed to the superior microstructure (inter-columnar void free) in the above potential range. In the potential range of -300 mV to + 350 mV both the coated substrates show passive behaviour even under

particle bombardment suggesting an immediate reformation/repair of the protective passive layer consisting of oxides and oxynitrides [19] of Chromium and Niobium. For the H-H coated substrates the protective nature of coating/passive layer is more evident, limiting the current densities to near constant values.

Erosion-corrosion is a complex phenomenon with a number of parameters affecting the combined wastage rates [20]. Factors such as particle type, size, shape, velocity, concentration in slurry, impact angle along with the chemical composition of the solution and electrochemical potentials have shown a marked effect on the total wastage rates and mechanisms of material removal [21]. Studies in the past have shown a synergistic effect between erosion and corrosion where corrosion assists mechanical wear in material removal [1, 22].

Figure 3

Figure 3 shows the volume loss measured by profiling erosion-corrosion wear scars. As observed, at all electrochemical potentials, except at +700 mV, the H-H coated specimens show lower volume loss as compared to the UBM coated specimens. The lower volume loss of H-H coated specimen can be attributed to higher hardness and superior microstructure (dense structure) with sharp interfaces between the multilayers of the coating. Lesser coating defects such as intercolumnar voids or macroparticle defects [9] will reduce the weak areas in the coating and will result in lower coating removal rate due to particle bombardment and hence enhanced corrosion and erosion-corrosion resistance of the coating in the conditions employed.

Consistent with the previous studies [4, 14] volume loss for the passivating potentials of +300 mV for both coatings was lower than at cathodic potentials of -1000 mV where no corrosion of specimen is expected. The results obtained suggest an antagonistic (negative synergism)

effect between erosion and corrosion [22]. The lower mass loss at +300 mV can be attributed to the protective nature of the passive layers of chromium (Cr) and niobium (Nb) formed in the electrochemical potential range of -300 mV and +350 mV [23]. Transport of the reacting species and corrosion reaction rates in the flowing fluid are higher [24] which can lead to the rapid reformation/repair of any passive layer being removed providing a cushioning effect to the incoming particles thereby reducing the total mass loss. These results are consistent with other studies where researchers have found that passive layer removal under solids-free impingement [24 - 25] and for conditions with suspended particles [26] depends on a critical value of velocity. Figure 4 shows the scanning electron microscopy images obtained with a Secondary Electron (SE) detector with a working distance of 5 cm. Results revealed that at the end of the experimentation, both the coatings were completely removed rendering the bare substrates with platelet type deformation as observed for erosion, and erosion-corrosion of "ductile" materials [18, 26, 27]. The scars on H-H coating, figure 4 (a-b), show different layers of the coating removed on the periphery thus suggesting a layer by layer coating removal mechanism. This is in contrast to the mechanism of abrupt coating removal by cracks linking between different macro defects observed as one of the dominant mechanisms for the ABS^{TM} deposited coatings [5].

Figure 4a and 4b

At +700 mV, both the coated specimens show increased volume loss as compared to the +300 mV. However the total volume loss is less as compared at "erosion only" conditions (-1000 mV) suggesting a limited interaction between erosion and corrosion at +700 mV. This limited synergistic effect [28 - 29] can be attributed to the preferential dissolution of the Cr phase [23] from the coating, figure 2 (potentials +600 mV onwards), tempered by the protective nature of the Nb passive layers which can provide a cushioning effect against the impacting particles thereby limiting the total volume loss [23]. EDX analysis of both the coatings exhibited that Cr concentration in the H-H coating (atomic weight 36%) was higher than the UBM (atomic

weight 32%) coating suggesting that the higher synergy in the H-H coating at +700 mV can be attributed to the Chromium rich stoichiometry of the coating which undergoes dissolution under erosion-corrosion conditions at such high potentials. It is estimated that this limited synergistic relation between erosion-corrosion for the H-H coating can be reduced by increasing the niobium content in the coating thereby improving its corrosion resistance, hardness and consequently erosion-corrosion resistance of the coating.

3.4: Erosion and corrosion contributions:

The total erosion-corrosion volume loss results obtained from the experiments can be further separated into individual contributions of erosion and corrosion [21],

$K_{EC} = K_E + K_C$ (i), which further can be divided as:

$K_E = K_{eo} + \Delta K_e$ (ii)

$K_C = K_{co} + \Delta K_c$ (iii)

where:

K_{EC} = Total volume loss due to erosion-corrosion (measured)

K_E = Volume loss due to erosion

K_{eo} = Volume loss in the absence of corrosion (measured under cathodic conditions)

ΔK_e = Change in erosion contribution due to corrosion

K_C = Volume loss due to corrosion (mathematically calculated)

K_{co} =Volume loss in the absence of erosion (calculated by Faraday's Law).

ΔK_c = Change in corrosion contribution due to erosion

Table 2

Table 2 signifies the individual contributions of erosion and corrosion for the coated substrates by HIPIMS and UBM coating technologies. As observed, at potentials + 300 mV and + 700 mV, the antagonistic effect of corrosion on erosion is clearly evident (negative ΔK_e values) where the passive layers lead to the reduced erosive wear of the coating. This effect is

more evident in the HIPIMS deposited coating suggesting superior coating microstructure than the UBM deposited coating. At potentials of + 700 mV, this antagonistic effect appears reduced due to the dissolution of Chromium from the coating, which can be addressed by increasing the niobium content of the coating in the future depositions.

4. Conclusions:

Nanoscale CrN/NbN multilayer were successfully deposited by HIPIMS and UBM technologies. Various microstructural characterisation and erosion-corrosion experiments indicated:

1. HIPIMS deposited (H-H coating) coatings exhibited enhanced wear, erosion, corrosion and hence erosion-corrosion resistance compared with the UBM deposited coatings in these conditions. Volume loss analysis at different corroding conditions, namely cathodic (-1000 mV) and passivating (+300 mV) showed that HIPIMS (H-H) coating outperformed the UBM coating, except at +700 mV (anodic) where the volume loss was approximately similar.
2. The superior erosion-corrosion resistance of the H-H coating could be attributed to the higher hardness and superior microstructure of the coating. Absence of growth defects such as droplet defects and inter-columnar voids together with dense structures (compared to that observed with the UBM technology) all contributed to the enhanced performance.
3. Passivating behaviour (+300 mV) of the nanoscale CrN/NbN multilayer coating led to negative synergism (antagonistic effect) between erosion and corrosion. Passivating conditions resulted in lower volume losses than in erosion only conditions.

References

[1] R.J.K. Wood, Wear 261 (9) (2006) 1012.

[2] P.E. Hovsepian, D.B. Lewis, W.-. Münz, Surface and Coatings Technology, 133-134 (2000) 166.

[3] W.-. Münz, F.J.M. Hauzer, D. Schulze, B. Buil, Surface and Coatings Technology 49 (1-3) (1991) 161.

[4] M.M. Stack, Y. Purandare, P. Hovsepian, Surface and Coatings Technology, 188-189 (2004) 556.

[5] Y. Purandare, M.M. Stack, P. Hovsepian, Wear, 259 (1-6) (2005) 256.

[6] V. Kouznetsov, K. Macák, J.M. Schneider, U. Helmersson, I. Petrov, Surface and Coatings Technology, 122 (2-3) (1999) 290.

[7] A.P. Ehiasarian, W.-. Münz, L. Hultman, U. Helmersson, I. Petrov, Surface and Coatings Technology 163-164 (2003) 267.

[8] C. Reinhard, A.P. Ehiasarian, P.E. Hovsepian, Thin Solid Films 515 (7-8) (2007) 3685.

[9] Y. P. Purandare, A. P. Ehiasarian and P. Eh. Hovsepian, J. Vac. Sci. Technol. 26 (2) (2008) 288.

[10] Arutiun P. Ehiasarian, P. E. Hovsepian, W.-D. Munz, USA patent, US 10718435, (2005)

[11] Arutiun P. Ehiasarian, Yolanda Aranda Gonzalvo, Terry D. Whitmore, Plasma Processes and Polymers 4 (S1) (2007) 309.

[12] A.C. Vlasveld, S.G. Harris, E.D. Doyle, D.B. Lewis, W.D. Munz, Surface and Coatings Technology 149 (2-3) (2002) 217.

[13] J.B. Zu, I.M. Hutchings, G.T. Burstein, Wear 140 (2) (1990) 331.

[14] Y.P. Purandare, M.M. Stack, P.E. Hovsepian, Surface and Coatings Technology, 201 (1-2) (2006) 361.

[15] Papken Eh. Hovsepian, Arutiun P. Ehiasarian, Yashodhan P. Purandare, Reinhold Braun, Ian M. Ross, Plasma Processes and Polymers, (2009) 200930412

[16] A. P. Ehiasarian, J. G. Wen, I. Petrov, J. Apply. Phys. 101 (2007) 054301.

[17] Scott Barnett and Anita Madan, Physics World (1998) 45.

[18] I. M. Hutchings, Tribology Friction and Wear of Engineering Materials, Butterworth-Heinemann, 1999.

[19] L. Thair, U. Kamachi Mudali, S. Rajagopalan, R. Asokamani, B. Raj, Corrosion Science 45 (9) (2003) 1951.

[20] M.M. Stack, S. Lekatos, F.H. Stott, Tribology International 28 (7) (1995) 445.

[21] M.M. Stack, S. Zhou, R.C. Newman, Wear 186-187 (Part 2) (1995) 523.

[22] M.M. Stack and N. Pungwiwat, Wear 256 (5) (2004) 565.

[23] Marcel Pourbaix, Atlas of Electrochemical Equilibria in Aqueous Solutions, NACE, 1966.

[24] B. Poulson, Wear 233-235 (1999) 497.

[25] A. Neville and T. Hodgkiess, Wear 233-235 (1999) 596.

[26] M.M. Stack, N. Corlett, S. Turgoose, Wear 255 (1-6) (2003) 225.

[27] A.V. Levy, Wear 108 (1) (1986) 1.

[28] M.M. Stack and T.M. Abd El-Badia, Wear 264 (9-10) (2008) 826.

[29] M.M. Stack and T.M. Abd El Badia, Wear 261 (11-12) (2006) 1181.

List of figure captions

Figure 1: TEM micrographs recorded in bright field mode: (a) low magnification cross-sectional view of the H-H coating showing base layer and through thickness coating (b) Nanoscale multilayer structure evident in the coating.

Figure 2: Current density curves obtained by polarising the specimens from -1000 mV to +1000 mV at a sweep rate of 1 mVs^{-1}.

Figure 3: Volume loss measured for nanoscale CrN/NbN multilayer coated substrates at different electrochemical potentials.

Figure 4: SEM micrographs of the erosion scars on H-H coatings eroded at -1000 mV (a) wear scar showing the periphery of the scar and exposed substrate (b) different layers of the coating visible at the periphery of the eroded area.

Figure 1a

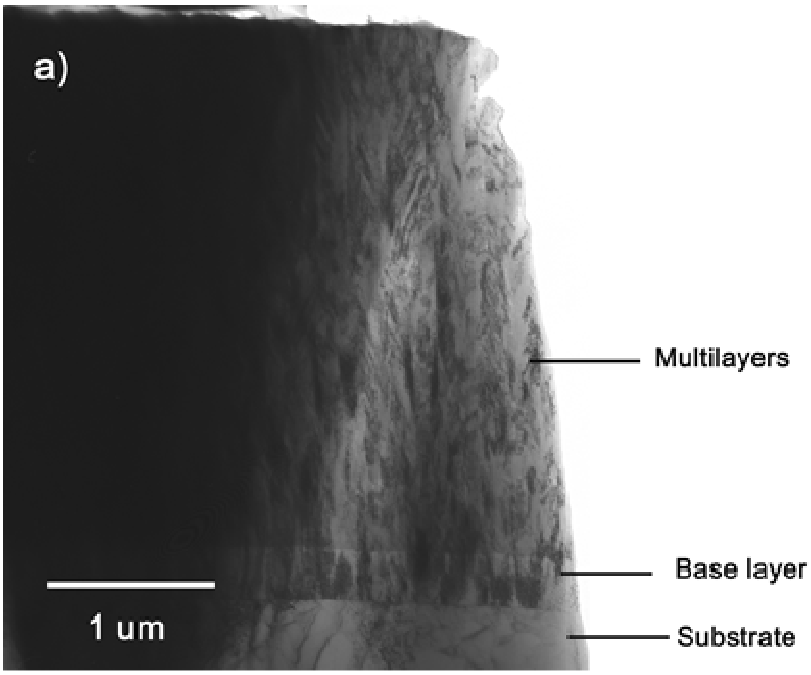

Figure1b

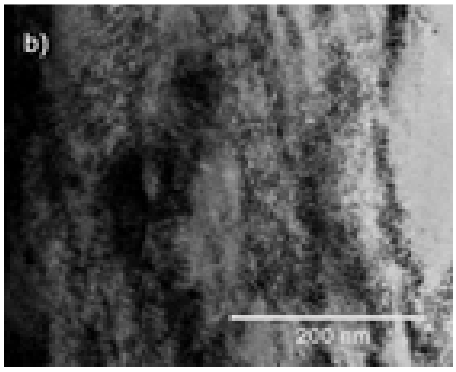

Figure 2

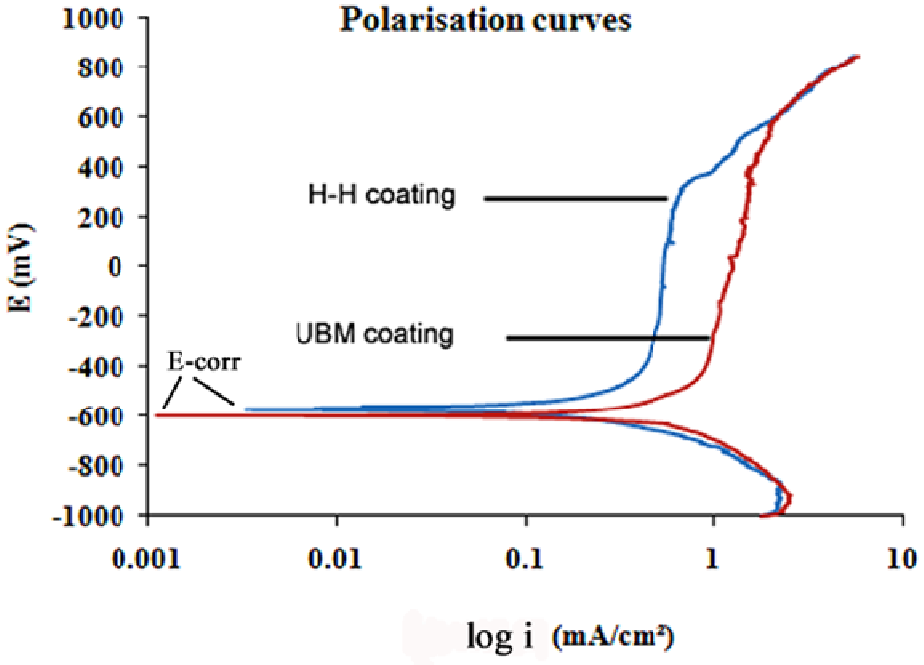

Figure 3

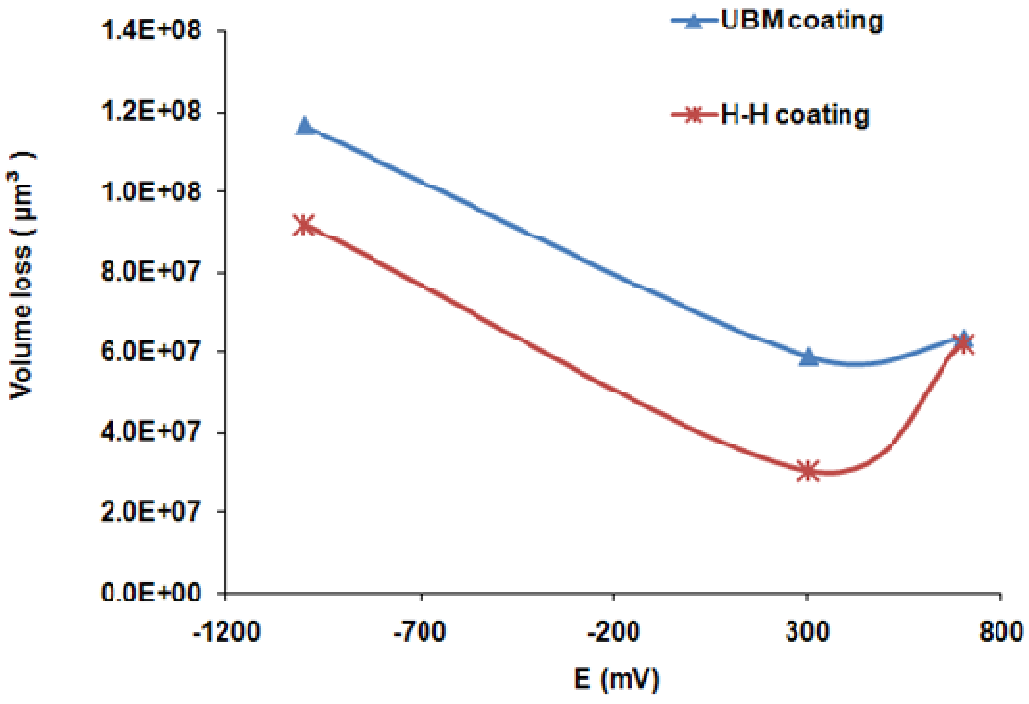

Figure 4a

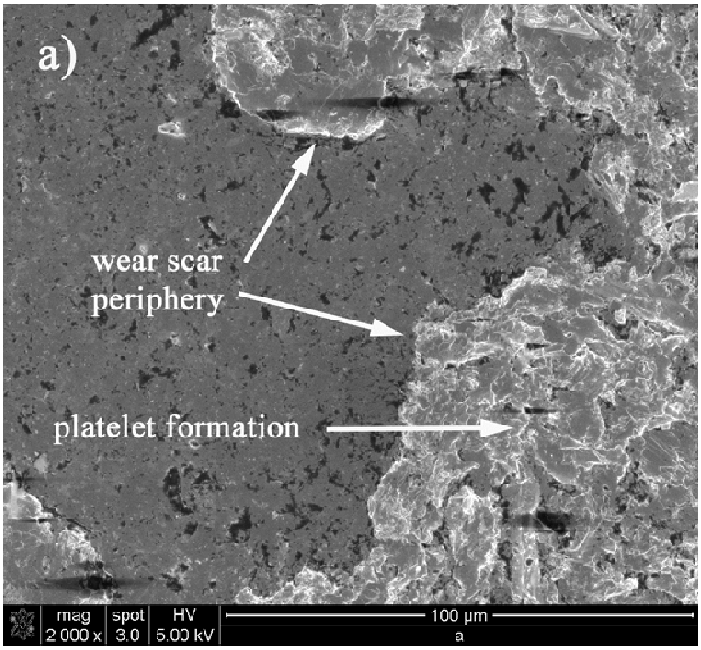

Figure 4b

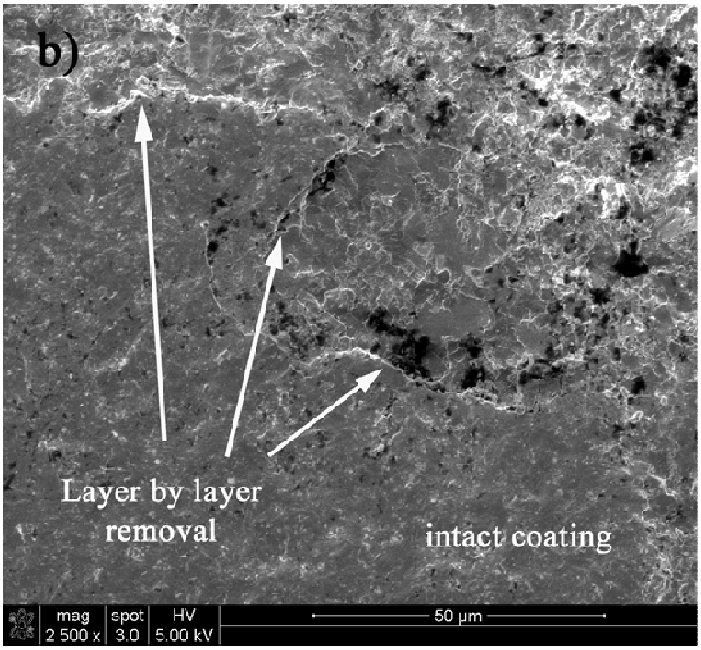

Table I: Summary of the coatings characterisation results.

Coating type	Bi-layer thickness (nm)	Residual Stress (GPa)	Micro hardness [$HK_{0.25N}$]	E [GPa]	Roughness (R_a)	Fric. Coeff. (μ)	Sliding wear [$m^3N^{-1}m^{-1}$] (x 10^{-15})	Nano hardness [GPa]
H-H	4.51	- 4.72 ± 0.56	3526 ± 30	381 ± 35	0.07 μm	0.46	1.22 ± 0.10	34 ± 4.2
UBM	2.38	- 1.59 ± 0.19	3049 ± 67	382 ± 59	0.04 μm	0.90	4.06 ± 0.13	31± 6.6

Table II: Individual contribution of erosion and corrosion calculated from the measured total erosion-corrosion volume loss.

Coating Technology	Corr. Potential (mV)	K_{EC}	K_E	K_C	K_{eo}	ΔK_e
HIPIMS-HIPIMS	**-1000**	-	9.17×10^7	-	9.17×10^7	-
	300	3.04×10^7	2.99×10^7	4.47×10^5	9.17×10^7	-6.18×10^7
	700	6.20×10^7	8.33×10^6	5.37×10^7	9.17×10^7	-8.34×10^7
HIPIMS-UBM	**-1000**	-	1.16×10^8	-	1.16×10^8	-
	300	5.89×10^7	5.00×10^7	8.87×10^6	1.16×10^8	-6.64×10^7
	700	6.36×10^7	1.84×10^7	4.52×10^7	1.16×10^8	-9.80×10^7